Trim21 regulates Nmi-IFI35 complex-mediated inhibition of innate antiviral response

Anshuman Das [a,b], Phat X. Dinh [a,b,1], Asit K. Pattnaik [a,b,*]

[a] School of Veterinary Medicine and Biomedical Sciences, University of Nebraska-Lincoln, Nebraska, USA
[b] Nebraska Center for Virology, University of Nebraska-Lincoln, Nebraska, USA

ARTICLE INFO

ABSTRACT

In this study, using an immunoprecipitation coupled with mass spectrometry approach, we have identified the E3 ubiquitin ligase Trim21 as an interacting partner of IFI35 and Nmi. We found that this interaction leads to K63-linked ubiquitination on K22 residue of Nmi, but not IFI35. Using domain deletion analysis, we found that the interaction is mediated via the coiled-coil domain of Nmi and the carboxyl-terminal SPRY domain of Trim21. Furthermore, we show that depletion of Trim21 leads to significantly reduced interaction of Nmi with IFI35, which results in the abrogation of the negative regulatory function of the Nmi-IFI35 complex on innate antiviral signaling. Thus, Trim21 appears to be a critical regulator of the functions of the Nmi-IFI35 complex. Overall, the results presented here uncover a new mechanism of regulation of the Nmi-IFI35 complex by Trim21, which may have implications for various autoimmune diseases associated uncontrolled antiviral signaling.

Introduction

The cellular innate immune response is an evolutionarily conserved mechanism to fight infections caused by invading pathogens. This response involves the activation of membrane bound Toll-like receptors (TLRs) or cytoplasmic sensors (RIG-I, MDA5 and STING) of foreign macromolecules including RNA and DNA. This leads to activation of a range of transcription factors such as IRF-3, IRF-5, IRF-7 and NF-kB, which can then induce a vast array of antiviral genes [interferon (IFN) stimulated genes or ISGs] or cytokines via stimulation of IFN synthesis (Egli et al., 2014; Randall and Goodbourn, 2008)

The innate immune pathways need to be tightly regulated by the host cells in order to prevent excessive IFN production that would otherwise be detrimental to the host. Some autoimmune diseases such as systemic lupus erythematosus (SLE) and rheumatoid arthritis are associated with unregulated innate immune response resulting from excessive production of type-I IFNs (James, 2014). Interestingly, some ISGs have been shown to function as negative regulators of the innate immune response by targeting various components of the signaling pathway (Richards and Macdonald, 2011). We recently reported that the ISG, interferon inducible protein 35 (IFI35), functions as a negative regulator of RIG-I signaling pathway by targeting RIG-I for proteasomal degradation (Das et al., 2014), although the host protein that ubiquitinates RIG-I in this IFI35-mediated negative regulatory pathway remains unidentified.

IFI35 is known to interact with the cellular protein, N-myc and STAT interacting protein (Nmi), another interferon-inducible protein (Zhou et al., 2000). Nmi was recently shown to negatively regulate virus-induced type-I IFN production by promoting K48-linked ubiquitination and proteasome-mediated degradation of IRF-7 (Wang et al., 2013). Although IFI35 and Nmi have been shown to be part of a high molecular mass complex (Chen et al., 2000), possibly comprising of other cellular proteins, it appears that they regulate the antiviral pathways by acting on different targets. Since, IFI35 and Nmi do not have any classical E3 ligase domains, it is possible that they recruit one or more E3 ubiquitin ligases to the complex to mediate their negative regulatory function on the innate antiviral pathways.

Among the various immune regulatory mechanisms, ubiquitination is one of the major forms of post-translational modifications that can positively or negatively regulate the innate immune response (Maelfait and Beyaert, 2012). The tripartite motif (Trim) proteins are a family of highly conserved E3 ubiquitin ligases, which conjugate ubiquitin on target proteins and have been shown to be important regulators of antiviral signaling (Versteeg et al., 2014). Trim proteins are defined by the presence of a conserved N-terminal RBCC motif whereas the C-terminus is variable. The RBCC motif contains the RING domain which is involved in catalyzing ubiquitin conjugation, the B-box domain which may aid in E2 ubiquitin ligase binding and stabilization, and the coiled-coil domain which is

required for homo and hetero-dimerization (Freemont, 2000). In the recent years, functional roles of various Trim proteins have been elucidated. One subset of Trim proteins that include Trim5, Trim14, Trim15, and Trim44 has been shown to positively regulate the antiviral response by ubiquitinating multiple targets in the pathway (Ottosson et al., 2006; Reymond et al., 2001; Uchil et al., 2013; Yang et al., 2013). On the other hand, Trim21, Trim27, Trim30 and Trim38 were recently shown to function as negative regulators of the antiviral response by mediating proteasomal degradation of various signaling factors (Higgs et al., 2008; Shi et al., 2008; Zhao et al., 2012; Zurek et al., 2012). Interestingly, some Trims like Trim21 are functionally flexible and can regulate the innate immune pathway in a positive or negative manner. Trim21 was first identified as an intracellular antibody receptor that can strongly bind to the Fc regions of antibodies found in complex with neutralized virus particles (Vaysburd et al., 2013). Later, Trim21 was shown to activate the NF-κB, AP-1 and IRF-3/7 mediated antiviral pathways by conjugating K63-linked ubiquitin chains whereas Trim21 was also recently found to down-regulate the DNA sensor DDX41 by K48-linked ubiquitination and subsequent proteasomal degradation (Zhang et al., 2013). Physiologically, Trim21 has been found to be an autoantigen in autoimmune diseases like rheumatoid arthritis, SLE and Sjogren's syndrome. Importantly, presence of antibodies against Trim21 are diagnostic markers of these diseases and their progression (James, 2014).

In our studies to further understand the role of IFI35 in regulating innate antiviral signaling, we have identified Trim21 as an interacting partner of IFI35 using an immunoprecipitation coupled with mass spectrometry approach. We show that Trim21 interacts with IFI35 as well as its partner protein, Nmi, but found that Trim21 conjugates K63-linked polyubiquitin chains exclusively on Nmi. We demonstrate that Trim21 mediated K63-linked ubiquitination of Nmi is required to form stable Nmi-IFI35 complex and also to promote the negative regulatory function of this complex on the innate antiviral response. Our results establish the role of Trim21 as a negative regulator of innate antiviral response by modulating the K63-linked ubiquitination of Nmi and its interaction with IFI35.

Results

Trim21 is an interacting partner of IFI35 and Nmi

To identify cellular factors that may regulate IFI35 function and thereby may promote the IFI35-mediated inhibition of the IFN response, we expressed 3xFlag-tagged IFI35 (3xFlag-IFI35) in 293T cells and performed immunoprecipitation (IP) using an anti-Flag antibody. The immunoprecipitates were separated by SDS-polyacrylamide gel electrophoresis (SDS-PAGE), silver-stained and the unique protein bands identified in the immunoprecipitates were subjected to liquid chromatography-mass spectrometry (LC-MS) analysis. From this analysis, we identified Trim21, which was present only in the immunoprecipitates of cells expressing the 3xFlag-IFI35 but not in cells transfected with the empty vector (Fig. 1A).
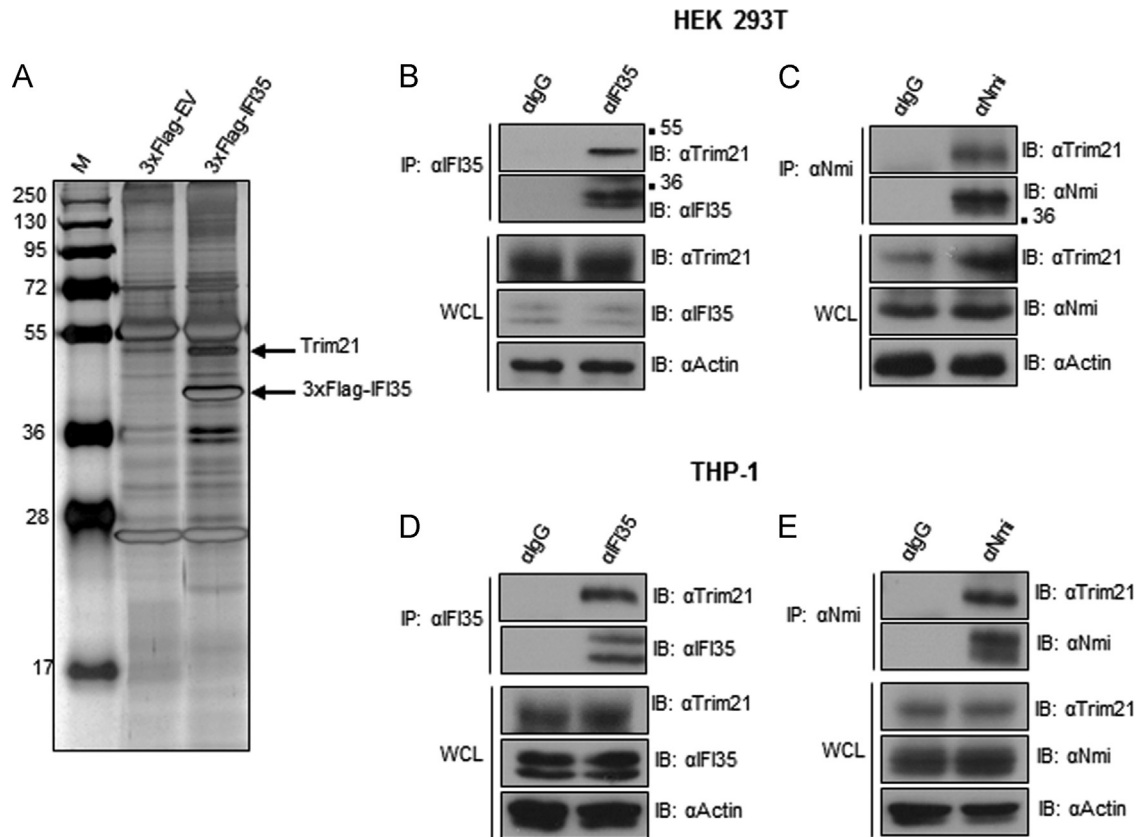

Fig. 1. Trim21 interacts with IFI35 and Nmi. (A) HEK 293T cells were transfected with 5 μg of 3xFlag-EV and 3xFlag-IFI35 plasmids. At 24 h post transfection (hpt), cell lysates were subjected to immunoprecipitation with anti-Flag monoclonal antibody (Mab), separated on 10% SDS-PAGE and silver stained. Molecular mass markers (in kDa) are shown in lane M. The bands containing Trim21 and 3xFlag-IFI35, as identified by LC-MS analysis, are indicated with arrows. (B) HEK 293T cell lysates were subjected to immunoprecipitation with anti-IFI35 antibody and immunoblotting with anti-Trim21 antibody. (C) HEK 293T cell lysates were subjected to immunoprecipitation with anti-Nmi antibody and immunoblotting with anti-Trim21 antibody. (D) THP-1 cell lysates were subjected to immunoprecipitation with anti-IFI35 antibody and immunoblotting with anti-Trim21 antibody. (E) THP-1 cell lysates were subjected to immunoprecipitation with anti-Nmi antibody and immunoblotting with anti-Trim21 antibody. Expression of the endogenous proteins in the whole cell lysates (WCLs) were analyzed by immunoblotting with the indicated antibodies. Approximate positions of the molecular weight markers (in kDa) are shown on the right side of the blots.
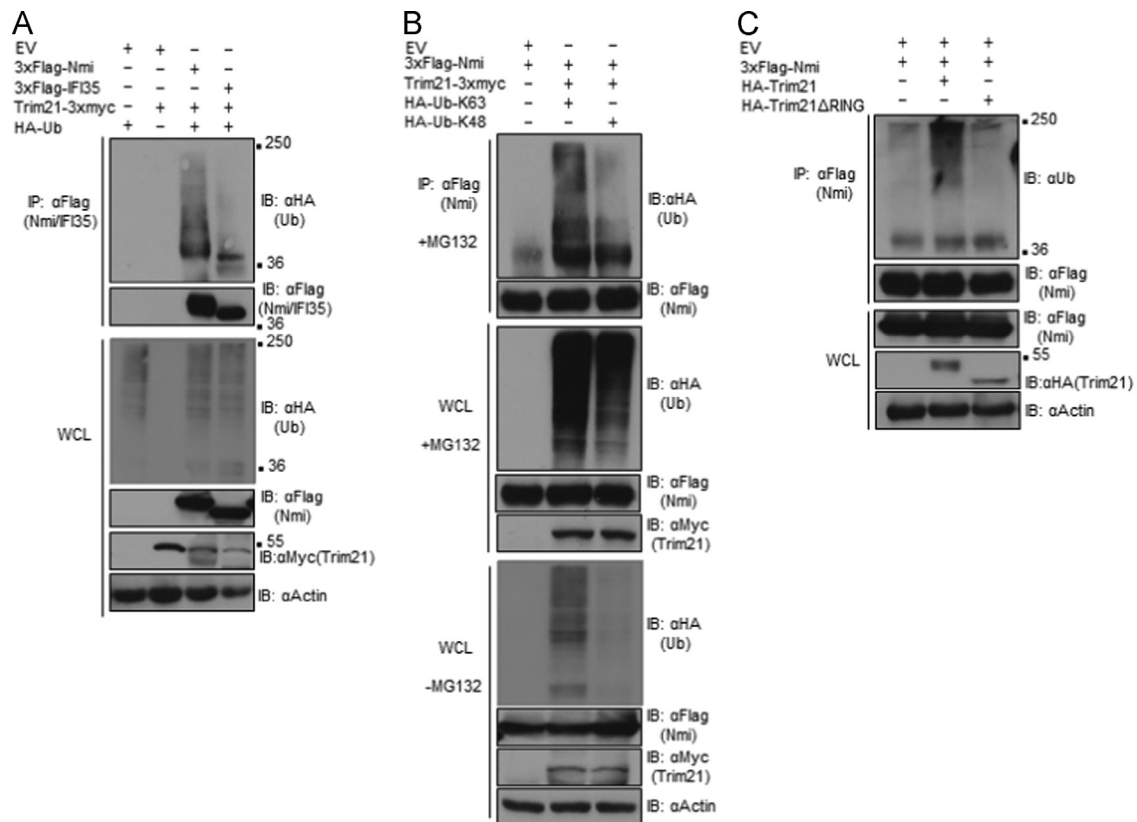
385

Fig. 2. Trim21 mediates K63-linked ubiquitination of Nmi. (A) HEK 293T cells were transfected with 1 μg each of 3xFlag-Nmi or 3xFlag-IFI35 along with 0.5 μg each of Trim21-3xMyc and HA-Ub. At 24 hpt, cell lysates were subjected to immunoprecipitation with anti-Flag polyclonal antibody. Ubiquitination of Nmi and IFI35 were detected using anti-HA Mab. Expression of proteins from transfected plasmids were analyzed in the WCLs using the indicated antibodies. (B) Cells were transfected with 1 μg of 3xFlag-Nmi along with 0.5 μg each of Trim21-3xMyc, HA-Ub-K63 or HA-Ub-K48 plasmids. At 24 hpt, cells were treated with 10 μM MG132 or equivalent amount of vehicle (DMSO) for 12 h and cell lysates were subjected to immunoprecipitation with anti-Flag polyclonal antibody. Ubiquitination of Nmi was detected using anti-HA Mab. Expression of proteins from transfected plasmids were analyzed in the MG132 treated and untreated WCLs using the indicated antibodies. (C) Cells were transfected with 1 μg of 3xFlag-Nmi along with 0.5 μg each of HA-Trim21 or HA-Trim21 ΔRING plasmids. At 24 hpt, cell lysates were subjected to immunoprecipitation with anti-Flag polyclonal antibody. Ubiquitination of Nmi was detected using anti-Ub antibody. Expression of proteins from transfected plasmids were analyzed in the WCLs using the indicated antibodies. Approximate positions of the molecular weight markers (in kDa) are shown on the right side of the blots.

To further confirm the interaction between Trim21 and IFI35, we performed co-immunoprecipitation of the endogenous proteins in 293T (non-immune) and THP-1 (immune) cells and found that the two proteins interact with each other in both cell types (Fig. 1B and D). We considered the possibility that this interaction may be mediated through other factors, as IFI35 is known to exist in high molecular mass complexes with the interferon-inducible N-Myc and STAT interactor (Nmi) (Chen et al., 2000; Zhou et al., 2000). Thus, we examined if any interaction exists between Trim21 and Nmi and found that the two proteins interact at the endogenous level in both the cell types (Fig. 1C and E). Overall, these results show that IFI35, Nmi, and Trim21 interact with each other and may form the high molecular mass complexes described previously for Nmi and IFI35.

Trim21 mediates K63-linked ubiquitination of Nmi

Since Trim21 is a well characterized E3 ubiquitin ligase shown to mediate auto-ubiquitination as well as ubiquitination of a variety of substrates (Oke and Wahren-Herlenius, 2012) for their degradation or activation, we first examined if Trim21 interaction with IFI35 and Nmi led to ubiquitination of these proteins. Interestingly, we observed significant ubiquitination of Nmi in cells overexpressing Trim21, but very low level of IFI35 ubiquitination was found under similar conditions (Fig. 2A). This suggests that although Trim21 interacts with both Nmi and IFI35, it primarily targets Nmi for ubiquitination. Since, Trim21 is known to mediate both K63- and K48-linked ubiquitination of substrates (McEwan et al., 2013; Zhang et al., 2013), we examined the type of ubiquitin linkage on Nmi by

over-expressing HA-tagged ubiquitin mutants (K48 only and K63 only) along with Trim21. Results show that Trim21 expression led to significant K63-linked ubiquitination but not K48-linked ubiquitination of Nmi (Fig. 2B). Furthermore, treatment of cells with the proteasomal inhibitor MG132 led to detection of minimal levels of K48-linked ubiquitination of Nmi (Fig. 2B), suggesting that Nmi primarily undergoes K63-linked ubiquitination in the presence of Trim21. Since K63-linked ubiquitination typically results in activation of target proteins (Davis and Gack, 2015), our data suggests that Nmi may be activated through this modification.

Trim21 belongs to the Trim family of proteins, many of which contain the tripartite motifs at their N-terminal RBCC domains (Ottosson et al., 2006; Reymond et al., 2001) that include a RING finger encoding E3 ubiquitin ligase (Freemont, 2000), a B-box and a coiled-coil domain mediating oligomerization. To demonstrate that the ubiquitination of Nmi was mediated specifically by Trim21 activity, we generated a catalytically inactive Trim21 mutant (Trim21ΔRING) and found that this mutant failed to ubiquitinate Nmi (Fig. 2C). Collectively, these data indicate that Trim21 mediates K63-linked ubiquitination of Nmi, which in turn may promote Nmi activation or its interaction with partner protein, IFI35.

Trim21 interacts with the coiled-coil domain of Nmi via its SPRY domain

To map the domains involved in the interaction between Trim21 and Nmi, we generated a series of deletion mutants of Trim21 and Nmi based on characterized functional domains of these proteins.

Nmi contains a coiled-coil (CC) domain at its amino-terminus and two N-myc interacting domains (NID1 and NID2) toward the carboxyl-terminus (Zhang et al., 2007b). These domains were individually deleted from the full-length Nmi as shown in Fig. 3A. Using co-IP assays, we found that deletion of the CC region of Nmi abrogated its interaction with Trim21, whereas NID1 and NID2 domain deletion mutants could still interact with Trim21 (Fig. 3B). This suggests that the CC domain of Nmi is essential for interaction with Trim21. Similarly, to identify the region(s) of Trim21 that interacts with Nmi, we deleted either the N-terminal RING (catalytic) domain, the central B-Box, the coiled-coil (CC) domain, the PRY and SPRY domains individually or together (Fig. 3C). Examination of interaction of these deletion mutants with Nmi showed that Trim21 lost interaction with Nmi only when SPRY domain was deleted (Fig. 3D). Overall, these data suggest that Trim21 requires its SPRY domain to interact with the CC region of Nmi.

Trim21 ubiquitines Nmi predominantly on lysine 22 residue

To identify the lysine residue(s) that are the targets of Trim21 mediated ubiquitination, we analyzed the Nmi amino acid sequence using an ubiquitination site prediction tool (http://www.ubpred.org). We found eight lysine (K) residues (at amino acid positions 5, 13, 22, 27, 56, 61, 176 and 183) of high and medium confidence, which could be potentially used for conjugation of ubiquitin chains. To identify the K residue(s) targeted by Trim21 for ubiquitination,

we initially constructed four double K mutants of Nmi (K5R/K13R, K22R/K27R, K56R/K61R, and K176R/K183R) by mutating the K residues into arginines (R). Since, we have previously shown (Fig. 2B) that Trim21 mediates K63-linked ubiquitination of Nmi, we tested these mutant Nmi constructs for their ability to be ubiquitinated by Trim21 via K63-linked ubiquitin chains. Our results show that mutation of both the K22 and K27 residues led to significantly reduced ubiquitination of Nmi (Fig. 4A). All the other double lysine mutants including the K176R/K183R mutant (in which the mutations are located outside of the CC domain), showed similar level of ubiquitination as the wild type (wt) protein. These data indicate that one or both of the K residues at positions 22 and 27 are required for Trim21 mediated ubiquitination of Nmi. To determine if one or both of these K residues are used for K63-linked ubiquitination, we generated single K22R and K27R mutants of Nmi and in a similar ubiquitination assay found that K22R mutant lost the ability to be ubiquitinated by Trim21, while the K27R mutant was ubiquitinated to similar extent as the wt protein (Fig. 4B). Collectively, these data suggest that the K22 of Nmi serves as the major acceptor site of K63-linked ubiquitination mediated by Trim21.

Trim21 is required for Nmi-IFI35 interaction

Previous reports have suggested that Nmi and IFI35 form steady state high molecular mass complexes, wherein Nmi prevents the proteasomal degradation of IFI35 (Chen et al., 2000). The identity of
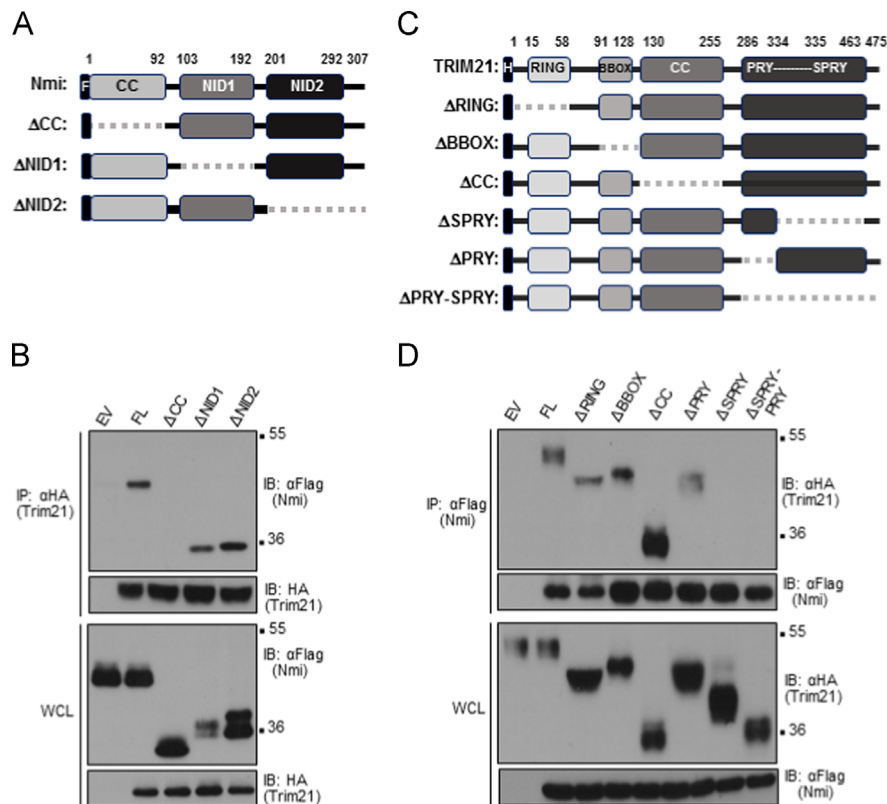

Fig. 3. Trim21 interacts with the coiled-coil domain of Nmi via its SPRY domain. (A) Schematic of the construction of domain deletion mutants of Nmi. F, Flag tag. Approximate amino acid positions of the domains are shown at the top. Various domains are boxed and discontinuous lines represent deletion of those regions. (B) The indicated domain deletion mutants of Nmi along with HA-Trim21 were transfected into HEK 293T cells. At 24 hpt, cell lysates were subjected to immunoprecipitation using anti-HA Mab. Interacting proteins were identified by immunoblotting with anti-Flag Mab. Expression of proteins from transfected plasmids were analyzed in the WCLs using the indicated antibodies. (C) Domain organization and deletion mutants of Trim21. H, HA tag. Approximate amino acid positions of the domains are shown at the top. Various domains are boxed and discontinuous lines represent deletion of those regions. (D) The indicated domain deletion mutants of Trim21 along with 3xFlag-Nmi were transfected into HEK 293T cells. At 24 hpt, cell lysates were subjected to immunoprecipitation using anti-Flag Mab. Interacting proteins were identified by immunoblotting with anti-HA Mab. Expression of proteins from transfected plasmids were analyzed in the WCLs using the indicated antibodies. Approximate positions of the molecular weight markers (in kDa) are shown on the right side of the blots.
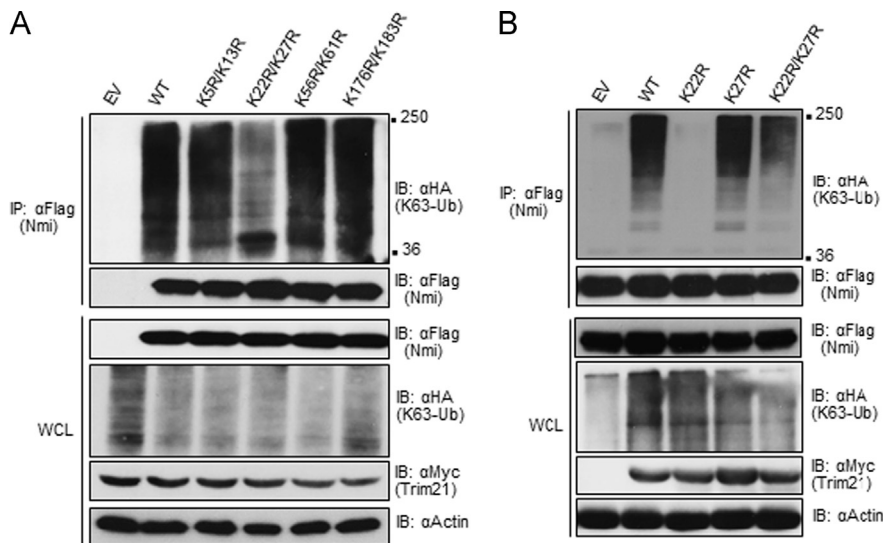
Fig. 4. Trim21 ubiquitinates Nmi on lysine 22 residue. (A) HEK 293T cells were transfected with 1 μg each of a panel of double lysine mutants of Nmi (Flag-tagged) along with 0.5 μg each of Trim21-3xMyc and HA-Ub-K63 plasmids. At 24 hpt, the cell lysates were subjected to immunoprecipitation using anti-Flag Mab. K63-linked ubiquitination of Nmi was detected using anti-HA Mab. Expression of the proteins from transfected plasmids were analyzed in the WCLs using the indicated antibodies. (B) Similar experiment was performed as described in panel A, except the single lysine mutants of Nmi were used. Approximate positions of the molecular weight markers (in kDa) are shown on the right side of the blots.

other cellular components, if any, in these high molecular mass complexes, is not known at this time; however, our findings that Trim21 interacts with both IFI35 and Nmi suggest that this E3 ubiquitin ligase maybe a part of this complex. Since, we have demonstrated that Trim21 ubiquitinates Nmi via K63-linkage, which in turn may activate Nmi function, we wondered if Trim21 also facilitates the interaction of Nmi and IFI35. To this end, we depleted the endogenous Trim21 using siRNAs and performed co-IP assays to determine if IFI35 and Nmi could still interact. Our results show that depletion of Trim21 led to significantly reduced interaction of Nmi with IFI35 (Fig. 5A). Likewise, when we performed immunoprecipitation with IFI35 antibody and immunoblotting with Nmi antibody, we detected significantly reduced level of Nmi being immunoprecipitated in cells depleted of Trim21 (Fig. 5B).

The above results were further strengthened with studies, wherein we transfected the siRNA-mediated Trim21-depleted cells with wt or a siRNA resistant mutant Trim21 (Trim21-siR) and examined the interaction of Nmi and IFI35. Indeed, the interaction of Nmi and IFI35 was restored in Trim21-depleted cells expressing the Trim21-siR but not in the cells expressing wt Trim21 (Fig. 5C), since, the exogenously and endogenously expressed wt Trim21 was depleted by the siRNA. Overall, these data suggest that Trim21 is required to facilitate the interaction of Nmi and IFI35 and likely plays a critical role in regulating the function(s) of the Nmi-IFI35 complex.

Trim21 regulates Nmi-mediated inhibition of the innate antiviral response

In a previous study, it was reported that Nmi promotes K48-linked ubiquitination and proteasome-mediated degradation of the transcription factor IRF-7, thereby inhibiting the innate antiviral signaling (Wang et al., 2013). Since, we found that Trim21 mediates K63-linked ubiquitination of Nmi, we asked if this modification in Nmi has any functional role in negative regulation of the antiviral response. To this end, we examined the levels of IFN-β (IFNB1) mRNA in 293T cells overexpressing the wt or the various K mutants (K22R, K27R and K22R/K27R) of Nmi. Our results showed that upon Sendai virus (SeV) infection to induce IFN synthesis, levels of IFN-β mRNA was about 4-fold lower in Nmi overexpressing cells compared to the control cells (empty vector transfected) not expressing

Nmi (Fig. 6A), indicating that Nmi overexpression suppresses IFN-β production. This is consistent with the previously described inhibitory role of Nmi on IFN production (Wang et al., 2013). Interestingly, the K22R mutant was unable to suppress IFN-β mRNA induction, whereas the K27R mutant suppressed IFN-β mRNA induction to levels similar to that observed with wt Nmi. The K22R/K27R double mutant moderately suppressed IFN-β mRNA levels (Fig. 6A). To examine if the establishment of an antiviral state (IFN-β production) was similarly affected in the cells expressing the wt and various mutant Nmi, we performed a VSV-IFN bioassay by examining the growth of GFP-tagged vesicular stomatitis virus (VSV-GFP) in 293T cells pretreated with supernatants from the experiment described in Fig. 6A. We found that VSV-GFP grew to higher titers in cells treated with supernatants from cells expressing wt or K27R mutant Nmi (9.7×10^5 pfu/ml and 8.7×10^5 pfu/ml, respectively) compared to that in cells treated with supernatants from empty vector transfected cells (1.5×10^5 pfu/ml). However, VSV-GFP growth was inhibited to similar extent in cells treated with supernatants from cells expressing K22R (4×10^5 pfu/ml) or K22R/K27R mutants (3.3×10^5 pfu/ml) (Fig. 6B). Together, these data suggest that K63-linked ubiquitination of Nmi at K22 but not K27, is important for its negative regulatory function on IFN production.

To further confirm these findings, we used specific siRNAs to deplete endogenous Trim21 in cells overexpressing Nmi and then quantified the IFN-β mRNA expression. In comparison to control siRNA (NT) transfected cells, SeV infection of Trim21 siRNA transfected cells led to significant induction of IFN-β mRNA in the presence of Nmi overexpression (Fig. 6C). Importantly, overexpression of a Trim21 siRNA resistant plasmid in cells treated with Trim21 siRNA could restore the Nmi- mediated suppression of IFN-β mRNA expression (Fig. 6C). The antiviral state of these cells was examined in a similar VSV-IFN bioassay as described for Fig. 6B. We observed that depletion of Trim21 in Nmi overexpressing cells led to reduced virus replication (2.4×10^5 pfu/ml) compared to control cells not depleted of Trim21 (8.7×10^5 pfu/ml). The suppression of virus replication was rescued in cells overexpressing the siRNA-resistant form of Trim21 (6.3×10^5 pfu/ml) (Fig. 6D). Taken together, these results suggest that Trim21 regulates Nmi-mediated inhibition of antiviral response by K63-linked ubiquitination of Nmi.

Discussion

This study advances our current understanding of an immune regulatory complex that includes the interferon stimulated genes Nmi, IFI35 and Trim21. Here, we have identified the E3 ubiquitin ligase, Trim21, as an interacting partner of IFI35 through an immunoprecipitation coupled with mass spectrometry screen. Interestingly, we found that Trim21 also interacts with Nmi, which is a known binding partner of IFI35. Both Nmi and IFI35 together have been shown to form a 200–300 kDa high molecular mass complex (Chen et al., 2000; Zhou et al., 2000). Various studies have identified several interacting partners of IFI35 and Nmi that maybe a part of the complex. Previous studies have shown B-ATF (member of AP-1 family of transcription factors) and CKIP-1 as interacting partners of IFI35 and Nmi and that these interactions were demonstrated to regulate antiviral gene transcription and cytokine response (Wang et al., 1996; Zhang et al., 2007b). Our recent work revealed an interaction between the cytoplasmic RNA sensor RIG-I and IFI35 and showed that this interaction resulted in down-regulation of RIG-I signaling due to K48-linked ubiquitination and degradation through

the proteasome machinery (Das et al., 2014). Here, we have shown that the interaction of Trim21 with Nmi and IFI35 occurs in non-immune (HEK 293T) as well as immune (THP-1) cells, indicating that the mechanism of Trim21-mediated regulation of Nmi-IFI35 complex may be relevant in both cell types.

In this work, we have uncovered a previously undescribed role of Trim21 in regulating the formation of Nmi-IFI35 complex by mediating K63-linked ubiquitination of Nmi. Based on our recent findings (Das et al., 2014), we initially hypothesized that Trim21 might be down-regulating RIG-I activation through K48-linked ubiquitination, although our studies did not reveal ubiquitination of RIG-I by Trim21 (data not shown). This is consistent with a report showing no change in RIG-I levels in cells overexpressing Trim21 (Zhang et al., 2013). Our previous observation that overexpression of IFI35 led to K48-linked ubiquitination and degradation of RIG-I suggests that yet another unidentified E3 ubiquitin ligase in association with IFI35 might be responsible for K48-linked ubiquitination of the RIG-I. Interestingly, here we found that although Trim21 interacts with both Nmi and IFI35, it primarily ubiquitinates Nmi. Furthermore, Trim21 may act as an intermediary molecule
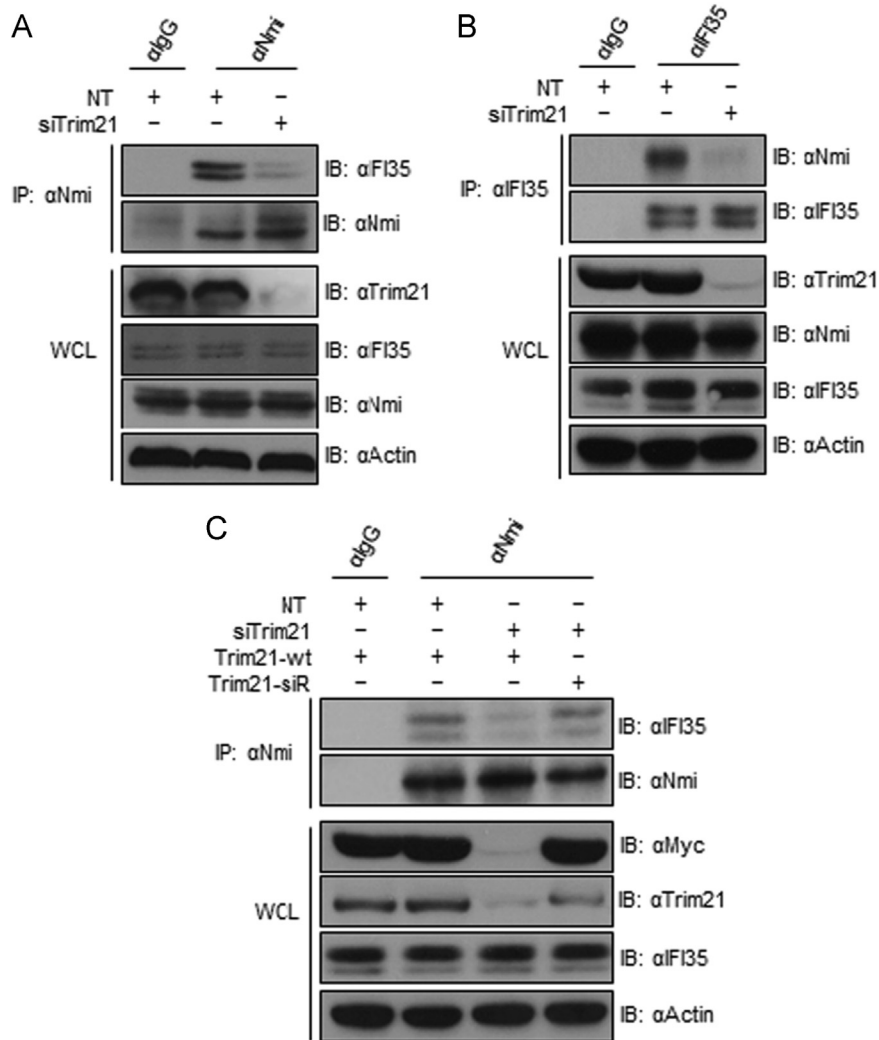

Fig. 5. Trim21 is required for Nmi-IFI35 interaction. (A) HEK 293T cells were transfected with 10 nM of control (NT) or Trim21 siRNA for 72 h. Cell lysates were subjected to immunoprecipitation with isotypic IgG control antibody or anti-Nmi antibody. Presence of endogenous IFI35 in the immunoprecipitates was detected by anti-IFI35 antibody. Endogenous expression of proteins in the WCLs was analyzed by using the indicated antibodies. (B) Similar experiment was performed as in panel A, except the cell lysates were subjected to immunoprecipitation with isotypic IgG control antibody or anti-IFI35 antibody. Presence of endogenous Nmi in the immunoprecipitates was detected by anti-Nmi antibody. (C) Cells were transfected with 10 nM of control (NT) or Trim21 siRNA (siTrim21) for 48 h. Subsequently, cells were re-transfected with 2 μg each of Myc-tagged wild-type Trim21 (Trim21-wt) or siRNA resistant mutant (Trim21-siR) plasmids for another 24 h. Finally, the cell lysates were subjected to immunoprecipitation with anti-Nmi antibody. Presence of endogenous IFI35 in the immunoprecipitates was detected by anti-IFI35 antibody. Expression of endogenous and exogenously expressed proteins in the WCLs was analyzed by using the indicated antibodies.
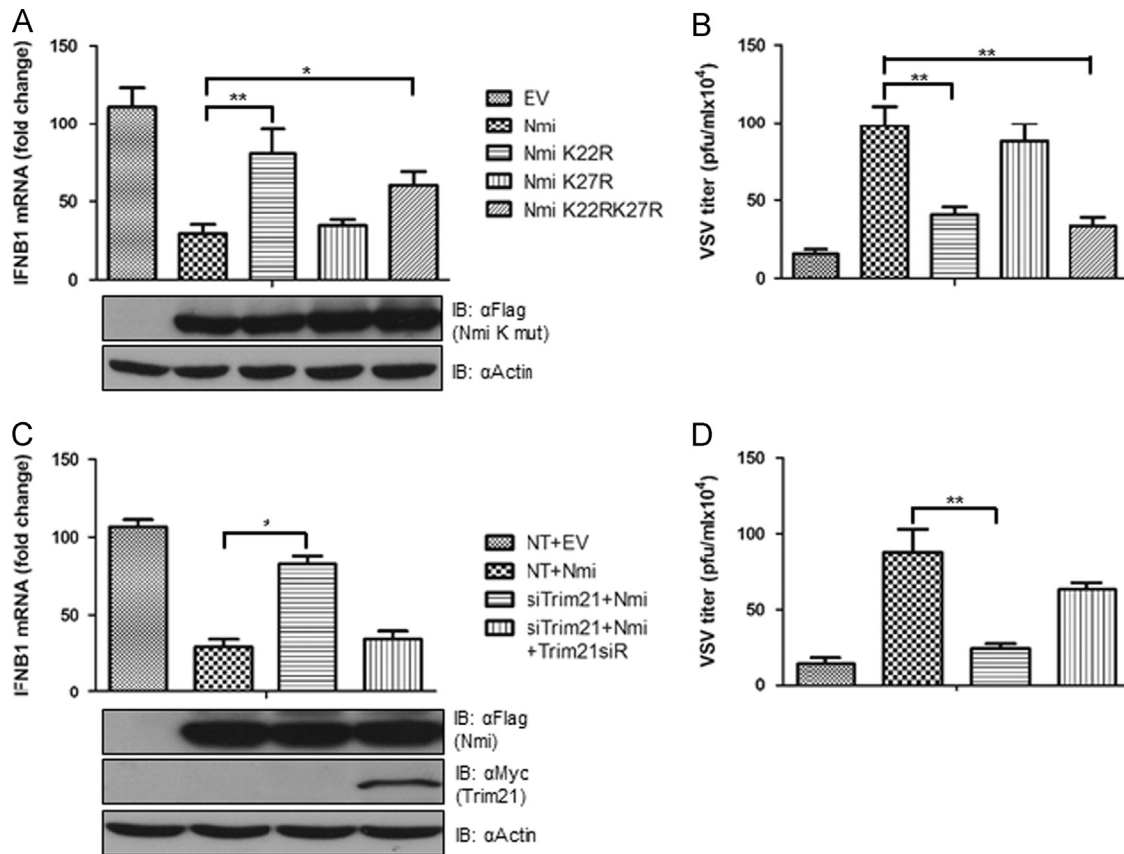
Fig. 6. Trim21 regulates Nmi-mediated inhibition of the innate antiviral response. (A) HEK 293T cells were transfected with an empty vector (EV) control or the indicated Nmi lysine mutants. At 24 hpt, these cells were infected with 80 HA units/ml of SeV for another 16 h. Finally, total RNA was extracted from these cells for qRT-PCR assay. IFNB1 and GAPDH mRNA levels were determined using specific Taqman primer and probes. Values were normalized to the internal control GAPDH and expressed as relative fold changes compared to mock-infected cells transfected with the EV. Expression of the Nmi lysine mutants (Nmi K mut) are shown in the immunoblots. Actin served as the loading control. (B) VSV-IFN bioassay. Supernatants from the experiment described in panel A, were UV-inactivated and added to fresh HEK 293T cells and incubated for 12 h. Then, cells were infected with 0.1 MOI VSV-GFP for another 16 h. Finally, the supernatants were used to determine VSV titers (pfu/ml) by plaque assay on BHK-21 cells. (C) Cells were transfected with 10 nM of NT or siTrim21 for 48 h. Subsequently, NT-transfected cells were re-transfected with an EV or Nmi encoding plasmids, whereas siTrim21-transfected cells were re-transfected with Nmi alone or in combination with Trim21-siR plasmids for another 24 h. Finally, IFNB1 mRNA was quantitated as described in panel A. Expression of Nmi and Trim21 are shown in the immunoblots. Actin served as the loading control. (D) Supernatants from the experiment described in panel C, were UV-inactivated, added to fresh HEK 293T cells and VSV-IFN bioassay was performed as described in panel B. Data presented in the panels are from three independent experiments and the values represent mean and SD for duplicate samples. $^*P < 0.05$, $^{**}P < 0.01$.

that facilitates the interaction of Nmi and IFI35, since depletion of Trim21 abrogates their interaction. The interaction of Trim21 and Nmi leads to conjugation of K63-linked ubiquitin chains on Nmi, which further facilitates the formation of Nmi-IFI35 complex.

The stability of Nmi appears to play important roles in cellular functions. It was previously reported that Tip60 (a histone acetyltransferase) enhances the stability of Nmi by preventing its proteasomal degradation, although the detailed mechanism remains unclear (Zhang et al., 2007a). Nmi has also been shown to confer stability of cellular proteins, for instance the association of Nmi with IFI35 in the high molecular mass complex is required to prevent proteasomal degradation of IFI35 (Chen et al., 2000). It is not clear what signals are necessary for degradation of IFI35; however, our results indicate a requirement for Trim21-mediated K63-linked ubiquitination of Nmi to facilitate interaction with IFI35 and possibly with other proteins in the complex. We did not observe any change in overall protein levels of Nmi or IFI35 when Trim21 was depleted (Fig. 5A and B), although the interaction of Nmi and IFI35 was significantly reduced. This suggests that K63-linked ubiquitination of Nmi is required to facilitate the interaction but does not affect stability of these proteins. Thus, our study highlights an important role of Trim21 in modulating the function of Nmi-IFI35 complex.

Trim21 is known to regulate function of various antiviral signaling proteins. A previous study demonstrated that Trim21
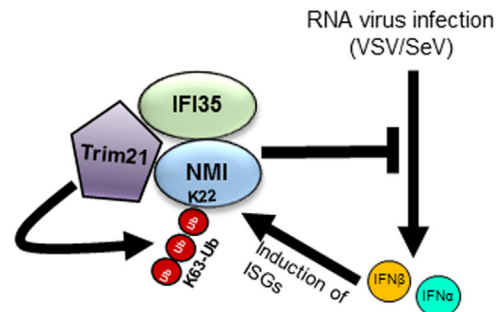

Fig. 7. Proposed model depicting the role of Trim21 in regulation of Nmi-mediated negative regulation of the innate antiviral response. Infection with RNA viruses like VSV or SeV leads to activation of the innate antiviral pathways, resulting in production of IFN-α/β, which in turn leads to induction of many ISGs including Trim21, Nmi and IFI35 as shown here. Trim21 interacts with both Nmi and IFI35 but primarily ubiquitinates Nmi on K22 residue via K63-linked ubiquitination. This facilitates interaction between Nmi with IFI35, which then in a negative feedback manner leads to inhibition of IFN-β production, resulting in an overall down-regulation of the innate antiviral signaling.

activates various components of IFN signaling pathway by conjugating K63-linked ubiquitin chains (McEwan et al., 2013). A recent study also found Trim21 as a negative regulator of DNA

sensing pathway by mediating K48-linked ubiquitination and degradation of the DNA sensor DDX41 (Zhang et al., 2013). Our data suggests that Trim21 functions as a negative regulator of antiviral signaling by modulating the activity of the Nmi-IFI35 complex (Fig. 7). We show that K63-linked ubiquitination of Nmi on the lysine 22 residue is required to maintain the negative regulatory function as mutation of the lysine to arginine leads to significantly higher antiviral response. Since, we measured the IFN-β mRNA levels as the readout for antiviral response, we cannot discern if Trim21 mediated K63-linked ubiquitination of Nmi negatively regulates only RIG-I/IRF-7 axis of signaling or other antiviral pathways as well. Thus, further work involving global pathway analysis using high-throughput platforms such as RNA-seq, may shed light on whether Trim21-mediated regulation of Nmi-IFI35 complex is a standalone mechanism or part of a larger regulatory network to control excessive IFN production.

Materials and methods

Cells, viruses and reagents

Human embryonic kidney HEK 293T cells were obtained from ATCC (Manassas, VA) and maintained in Dulbecco's modified Eagle's medium (DMEM) supplemented with 10% fetal bovine serum (FBS) and the antibiotics (PKS): penicillin (100 units/ml), kanamycin (20 units/ml) and streptomycin (20 units/ml). Baby hamster kidney (BHK-21) cells were maintained in modified Eagle's medium (MEM) supplemented with 5% FBS and 1X PKS. THP-1 cells (gift from Dr. Tom Petro, University of Nebraska Medical Center) were maintained in Roswell Park Memorial Institute Medium (RPMI) supplemented with 10% FBS, 1X PKS and 1 mM sodium pyruvate. MG132 was purchased from Cayman Chemicals (Ann Arbor, MI).

Sendai virus (SeV) Cantell strain was purchased from Charles River laboratories. SeV infections were performed at 80 haemagglutinin units per ml (HA units/ml) for 16 hours (h). Stocks of VSV-GFP were prepared in the lab as described previously (Dinh et al., 2011). For the VSV-IFN bioassay, HEK 293T cells were infected with VSV-GFP at an MOI of 0.1 plaque forming unit (PFU) per cell for 14 h. Virus titers were determined by plaque assays on BHK-21 cells.

Antibodies

Anti-Flag mouse monoclonal antibody (Mab; clone M2), anti-Flag and anti-HA rabbit polyclonal antibodies were purchased from Sigma Aldrich Inc. Anti-HA (mouse Mab; clone HA.11) was purchased from Covance Inc. Anti-c-Myc (clone 9E1; sc-40), anti-Actin (sc-47778), anti-IFI35 (sc-100769), anti-Nmi (sc-101100), anti-Ub (sc-8017) and anti-Trim21 (sc-25351) Mabs were purchased from Santa Cruz Biotechnology Inc. HRPO-conjugated goat anti-mouse (A4416) and goat anti-rabbit (A6154) antibodies were purchased from Sigma Aldrich Inc. For immunofluorescent staining, Alexa Fluor 488-conjugated donkey anti-mouse IgG (A21202), Alexa Fluor 647-conjugated donkey anti-rabbit IgG (A-31573) were purchased from Life Technologies Inc.

Plasmid constructs

3xFlag-IFI35 construct has been described previously (Das et al., 2014). 3xFlag-Nmi was constructed in a similar manner by cloning PCR amplified Nmi cDNA from 293T cells into a modified pcDNA-3xFlag vector at the KpnI and NotI sites. The Nmi domain deletion mutants namely ΔCC (Δ1–92), ΔNID1 (Δ103–192) and ΔNID2 (Δ201–292) were constructed on the 3xFlag-Nmi background using the Phusion site-directed mutagenesis approach (Thermo Scientific). A panel of double lysine (K) mutants of 3xFlag-Nmi namely

Table 1
Primers used in this study.

Primer name	Sequence (5′ to 3′)	Purpose
ΔCC-R	GGTACCAAGCTTGTCATCG	Construction of Nmi ΔCC mutant
ΔCC-F	AGCTCGAAAGTTCCTTATGAG	
ΔNID1-R	TTTTTGTATCTCATAAGGAACTTTCG	Construction of Nmi ΔNID1 mutant
ΔNID1-F	CGCGTGGACTATGACAGAC	
ΔNID2-R	GGACTGTCTGTCATAGTCC	Construction of Nmi ΔNID2 mutant
ΔNID2-F	GTCAAGTGTTCTCTAGGTCAAC	
Nmi KpnI-F	ATATATGGTACCATGGAAGCTGATAAAGATGAC	Construction of 3xFlag-Nmi
Nmi NotI-R	ATATATGCGGCCGCCTATTCTTCAAAGTATGCTATG	
ΔRING-R	GACCTCCTCCCACATCATTG	Construction of Trim21 ΔRING mutant
ΔRING-F	CTGCTCAAGAATCTCCGGC	
ΔBBOX-R	TTCCCCCTGTGTGCCCTC	Construction of Trim21 ΔBBOX mutant
ΔBBOX-F	GAGGAGGCTGCACAGGAG	
ΔSPRY-R	ACATGTCCTCAGCATCTTCTTC	Construction of Trim21 ΔSPRY-PRY mutant
ΔSPRY-F	CCACTGAATATTGGATCACAAGG	
Trim21sires-F	GTCCTGTGTGTCGACAACGTTTCCTACTTAAGAATCTCCG	Construction of Trim21 siRNA resistant mutant
Trim21sires-R	AGACGCTGCCCCCACCTTTCCCAACC	
K5RK13R-F	CTGATAGAGATGCACACAACAAATTCTTAGGGAGC	Construction of Nmi K5/K13 double mutant
K5RK13R-R	CTTCCATGGTACCAAGCTTGTCATCGTC	
K22RK27R-F	GAATTTATAAGAGATGAACAAAATAGGGGAC	Construction of Nmi K22/K27 double mutant
K22RK27R-R	ATCTGGCGAATGCTCCTTAAGAATTTG	
K56RK61R-F	CTACCAGAGAATTCCAGATTAGAGAGG	Construction of Nmi K56/K61 double mutant
K56RK61R-R	CCTCTTGTAACTCCGTTTCAAGC	
K176RK183R-F	GAGACAGACTAGAGCTGAGCTTTTCAAGGTCCCG	Construction of Nmi K176/K183 double mutant
K176RK183R-R	TCATTTGATCTTCACGCAATGTGTCAGG	
K22R-F	GAATTTATAAGAGATGAACAAAATAAGGGAC	Construction of Nmi K22 mutant
K22RK27R-R	ATCTGGCGAATGCTCCTTAAGAATTTG	
K27R-F	GAATTTATAAAAGATGAACAAAATAGGGGAC	Construction of Nmi K27 mutant
K22RK27R-R	ATCTGGCGAATGCTCCTTAAGAATTTG	
Trim21 KpnI-F	ATATGGTACCATGGCTTCAGCAGCACGCTTG	Construction of HA-Trim21
Trim21 NotI-R	ATATGCGGCCGCTCAATAGTCAGTGGATCCTTGTG	
Trim21 KpnI-F	ATATGGTACCATGGCTTCAGCAGCACGCTTG	Construction of Trim21-3xmyc
Trim21NS NotI-R	ATATGCGGCCGCATAGTCAGTGGATCCTTGTGATC	

K5R/K13R, K22R/K27R, K56R/K61R, K176R/K183R and single K mutants namely K22R and K27R were generated using the Phusion site-directed mutagenesis approach. The mutagenic primers used to mutate the K residues to R are listed in Table 1. Trim21 tagged with HA at the N-terminus (HA-Trim21) was constructed by cloning PCR amplified Trim21 cDNA from 293T cells into a modified pcDNA vector with HA-tag (pcDHA) at the KpnI and NotI sites. HA-Trim21 was used as a template to generate the domain deletion mutants, namely, ΔRING (Δ15–58), ΔBBOX (Δ91–128), ΔCC (Δ130–255), ΔPRY (Δ286–334), ΔSPRY (Δ335–463) and ΔSPRY-PRY (Δ286–463). A C-terminus 3xMyc tagged Trim21 (Trim21-3xMyc) was also generated by cloning PCR amplified Trim21 cDNA from 293T cells into pA3xmyc vector [gift from Dr. Charles Wood, University of Nebraska−Lincoln (UNL)] at the KpnI and NotI sites. A Trim21 siRNA resistant plasmid (Trim21-3xMyc-siR) was constructed by mutating the siRNA target region (nt positions 162–182 in the Trim21 ORF) using the mutagenic primers (Table 1). N-terminus HA-tagged ubiquitin was expressed from pMT123-HA-Ubiquitin plasmid which has been described previously (Treier et al., 1994). pRK5-HA-Ubiquitin K48 (17605) and pRK5-HA-Ubiquitin K63 (17606) (Lim et al., 2005) were purchased from Addgene.

siRNA-mediated silencing

To deplete the endogenous Trim21, we transfected Trim21 siRNA duplex 2 from Qiagen (Qiagen # SI00048251) at a concentration of 10 nM into 293T cells and incubated for 48–72 h. Similar concentration of non-targeting (NT) siRNA (Qiagen # 1027281) was used as negative control. The depletion was confirmed by immunoblotting using antibody against endogenous Trim21 (sc-25351). For determination of IFN-β mRNA levels, quantitative Real Time PCR (qRT-PCR) was performed. Total cellular RNA was extracted using Trizol (Invitrogen) according to manufacturer's protocol. First strand cDNA was synthesized with 2 μg of total RNA using M-MLV reverse transcriptase (Invitrogen) according to manufacturer's protocol. The cDNA was diluted 2-fold and 100 ng of cDNA was used for each qRT-PCR reaction. Taqman primers and probe mix (20X) for IFNB1 or IFN-β (Hs01077958), GAPDH (Hs99999905) and Taqman Gene expression master mix (2X) (Applied Biosystems) were added along with cDNA and water to a final volume of 20 μL per well. qRT-PCR reaction was carried out in MicroAmp optical 96 well plates using the Step One Plus Real Time PCR system (Applied Biosystems). The standard protocol for Taqman based qRT-PCR provided by the manufacturer was used. Relative fold changes in gene expression were automatically calculated by the Step One Plus Real Time PCR system software (Applied Biosystems) following the $\Delta\Delta$CT method.

Plasmid transfections and western blotting

Transfection of HEK 293T cells with plasmids was performed using Lipofectamine 2000 (Invitrogen) as per manufacturer's instructions. Usually, 12 h after transfection, the cells were washed and fresh growth media was added and incubated for 24–48 h. For western blotting assays, dilutions of primary antibodies used were as follows: anti-Flag MabM2 (1:4000), anti-HA Mab (1:4000), anti-Myc Mab (1:2000), anti-Trim21 (1:1000), anti-Nmi (1:1000), anti-IFI35 (1:1000), anti-Ub (1:2000) and anti-Actin (1:5000). The corresponding HRPO conjugated secondary antibodies were used at dilutions ranging from (1:2000 to 1:5000).

Co-immunoprecipitation (Co-IP) assay

For interaction experiments, 6-well plates containing 70–80% confluent 293T cells were transfected with plasmids and incubated for 24 h. Following incubation, cells were lysed in radio-immunoprecipitation buffer without SDS (ROS lysis buffer),

whose composition has been described earlier (Dinh et al., 2011). The lysates were clarified by low speed centrifugation (15,000g) for 20 min at 4 °C and incubated with the primary antibody overnight after which 4 mg of protein A-Sepharose beads (GE Healthcare Bioscience AB) washed 3 times in the ROS lysis buffer was added to each sample and incubated for 2–4 h. Beads with bound immune complexes were thoroughly washed at least 3 times with the lysis buffer, 20–30 μl 2X SDS-polyacrylamide gel electrophoresis (PAGE) sample preparation buffer was added, boiled for 5 min and the proteins in the eluted samples were resolved in 10% SDS-polyacrylamide gel. Subsequently, the proteins were transferred to polyvinylidene difluoride (PVDF) membrane and immunoblotting was carried out using antibodies as described in the western blotting section.

Silver staining and mass spectrometric (MS) analysis of proteins

For MS analysis, the immunoprecipitated proteins were separated by SDS-PAGE, the proteins were stained using the silver staining method described previously (Dinh et al., 2011), and the selected bands were excised from the stained gel for liquid chromatography-mass spectrometry (LC−MS) analysis. Briefly, individual gel pieces containing the protein(s) were digested by trypsin and the digested peptides were extracted in 5% formic acid−50% acetonitrile and separated using a C_{18} reversed-phase LC column (75 μm by 15 cm; BEH 130, 1.7 μm, Waters, Milford, MA). A quantitative time of flight (Q-TOF) Ultima tandem mass spectrometer with electrospray ionization (Waters) was used to analyze the eluting peptides. The peak lists of MS/MS data were generated using Distiller (Matrix Science, London, United Kingdom) with charge state recognition and deisotoping with the other default parameters for Q-TOF data. Data base searches of the acquired MS/MS spectra were performed using Mascot (Matrix Science, v2.2.0, London, United Kingdom).

Statistical analysis

Graphs were generated and statistical analyses were performed using Graph Pad Prism software (Graph Pad software Inc.). Statistical significance between groups was determined by two-tailed paired Student's t test. $P < 0.05$ was considered statistically significant.

References

Chen, J., Shpall, R.L., Meyerdierks, A., Hagemeier, M., Bottger, E.C., Naumovski, L., 2000. Interferon-inducible Myc/STAT-interacting protein Nmi associates with IFP 35 into a high molecular mass complex and inhibits proteasome-mediated degradation of IFP 35. J. Biol. Chem. 275, 36278–36284.

Das, A., Dinh, P.X., Panda, D., Pattnaik, A.K., 2014. Interferon-inducible protein IFI35 negatively regulates RIG-I antiviral signaling and supports vesicular stomatitis virus replication. J. Virol. 88, 3103–3113.

Davis, M.E., Gack, M.U., 2015. Ubiquitination in the antiviral immune response. Virology 479-480, 52–65.

Dinh, P.X., Beura, L.K., Panda, D., Das, A., Pattnaik, A.K., 2011. Antagonistic effects of cellular poly(C) binding proteins on vesicular stomatitis virus gene expression. J. Virol. 85, 9459–9471.

Egli, A., Santer, D.M., O'Shea, D., Tyrrell, D.L., Houghton, M., 2014. The impact of the interferon-lambda family on the innate and adaptive immune response to viral infections. Emerg. Microbes Infect. 3, e51.

Freemont, P.S., 2000. RING for destruction? Curr. Biol.: CB 10, R84–87.

Higgs, R., Ni Gabhann, J., Ben Larbi, N., Breen, E.P., Fitzgerald, K.A., Jefferies, C.A., 2008. The E3 ubiquitin ligase Ro52 negatively regulates IFN-beta production post-pathogen recognition by polyubiquitin-mediated degradation of IRF3. J. Immunol. 181, 1780–1786.

James, L.C., 2014. Intracellular antibody immunity and the cytosolic Fc receptor TRIM21. Curr. Top. Microbiol. Immunol. 382, 51–66.

Lim, K.L., Chew, K.C., Tan, J.M., Wang, C., Chung, K.K., Zhang, Y., Tanaka, Y., Smith, W., Engelender, S., Ross, C.A., Dawson, V.L., Dawson, T.M., 2005. Parkin mediates nonclassical, proteasomal-independent ubiquitination of synphilin-1: implications for Lewy body formation. J. Neurosci. 25, 2002–2009.

Maelfait, J., Beyaert, R., 2012. Emerging role of ubiquitination in antiviral RIG-I signaling. Microbiol. Mol. Biol. Rev. 76, 33–45.

McEwan, W.A., Tam, J.C., Watkinson, R.E., Bidgood, S.R., Mallery, D.L., James, L.C., 2013. Intracellular antibody-bound pathogens stimulate immune signaling via the Fc receptor TRIM21. Nat. Immunol. 14, 327–336.

Oke, V., Wahren-Herlenius, M., 2012. The immunobiology of Ro52 (TRIM21) in autoimmunity: a critical review. J. Autoimmun. 39, 77–82.

Ottosson, L., Hennig, J., Espinosa, A., Brauner, S., Wahren-Herlenius, M., Sunnerhagen, M., 2006. Structural, functional and immunologic characterization of folded subdomains in the Ro52 protein targeted in Sjogren's syndrome. Mol. Immunol. 43, 588–598.

Randall, R.E., Goodbourn, S., 2008. Interferons and viruses: an interplay between induction, signalling, antiviral responses and virus countermeasures. J. Gen. Virol. 89, 1–47.

Reymond, A., Meroni, G., Fantozzi, A., Merla, G., Cairo, S., Luzi, L., Riganelli, D., Zanaria, E., Messali, S., Cainarca, S., Guffanti, A., Minucci, S., Pelicci, P.G., Ballabio, A., 2001. The tripartite motif family identifies cell compartments. EMBO J. 20, 2140–2151.

Richards, K.H., Macdonald, A., 2011. Putting the brakes on the anti-viral response: negative regulators of type I interferon (IFN) production. Microbes Infect. 13, 291–302.

Shi, M., Deng, W., Bi, E., Mao, K., Ji, Y., Lin, G., Wu, X., Tao, Z., Li, Z., Cai, X., Sun, S., Xiang, C., Sun, B., 2008. TRIM30 alpha negatively regulates TLR-mediated NF-kappa B activation by targeting TAB2 and TAB3 for degradation. Nat. Immunol. 9, 369–377.

Treier, M., Staszewski, L.M., Bohmann, D., 1994. Ubiquitin-dependent c-Jun degradation in vivo is mediated by the delta domain. Cell 78, 787–798.

Uchil, P.D., Hinz, A., Siegel, S., Coenen-Stass, A., Pertel, T., Luban, J., Mothes, W., 2013. TRIM protein-mediated regulation of inflammatory and innate immune signaling and its association with antiretroviral activity. J. Virol. 87, 257–272.

Vaysburd, M., Watkinson, R.E., Cooper, H., Reed, M., O'Connell, K., Smith, J., Cruickshanks, J., James, L.C., 2013. Intracellular antibody receptor TRIM21 prevents fatal viral infection. Proc. Natl. Acad. Sci. USA 110, 12397–12401.

Versteeg, G.A., Benke, S., Garcia-Sastre, A., Rajsbaum, R., 2014. InTRIMsic immunity: positive and negative regulation of immune signaling by tripartite motif proteins. Cytokine Growth Factor Rev. 25, 563–576.

Wang, J., Yang, B., Hu, Y., Zheng, Y., Zhou, H., Wang, Y., Ma, Y., Mao, K., Yang, L., Lin, G., Ji, Y., Wu, X., Sun, B., 2013. Negative regulation of virus-triggered type I IFN production by targeting IRF7. J. Immunol. 191, 3393–3399.

Wang, X., Johansen, L.M., Tae, H.J., Taparowsky, E.J., 1996. IFP 35 forms complexes with B-ATF, a member of the AP1 family of transcription factors. Biochem. Biophys. Res. Commun. 229, 316–322.

Yang, B., Wang, J., Wang, Y., Zhou, H., Wu, X., Tian, Z., Sun, B., 2013. Novel function of Trim44 promotes an antiviral response by stabilizing VISA. J. Immunol. 190, 3613–3619.

Zhang, K., Zheng, G., Yang, Y.C., 2007a. Stability of Nmi protein is controlled by its association with Tip60. Mol. Cell Biochem. 303, 1–8.

Zhang, L., Tang, Y., Tie, Y., Tian, C., Wang, J., Dong, Y., Sun, Z., He, F., 2007b. The PH domain containing protein CKIP-1 binds to IFP35 and Nmi and is involved in cytokine signaling. Cell Signal 19, 932–944.

Zhang, Z., Bao, M., Lu, N., Weng, L., Yuan, B., Liu, Y.J., 2013. The E3 ubiquitin ligase TRIM21 negatively regulates the innate immune response to intracellular double-stranded DNA. Nat. Immunol. 14, 172–178.

Zhao, W., Wang, L., Zhang, M., Wang, P., Yuan, C., Qi, J., Meng, H., Gao, C., 2012. Tripartite motif-containing protein 38 negatively regulates TLR3/4- and RIG-I-mediated IFN-beta production and antiviral response by targeting NAP1. J. Immunol. 188, 5311–5318.

Zhou, X., Liao, J., Meyerdierks, A., Feng, L., Naumovski, L., Bottger, E.C., Omary, M.B., 2000. Interferon-alpha induces nmi-IFP35 heterodimeric complex formation that is affected by the phosphorylation of IFP35. J. Biol. Chem. 275, 21364–21371.

Zurek, B., Schoultz, I., Neerincx, A., Napolitano, L.M., Birkner, K., Bennek, E., Sellge, G., Lerm, M., Meroni, G., Soderholm, J.D., Kufer, T.A., 2012. TRIM27 negatively regulates NOD2 by ubiquitination and proteasomal degradation. PLoS One 7, e41255.